PCCP

Accepted Manuscript

ROYAL SOCIETY OF CHEMISTRY

www.rsc.org/pccp

Phys. Chem. Chem. Phys.

RSCPublishing

ARTICLE

A femtosecond study of the anomaly in electron injection for dye-sensitized solar cells: Influence of isomerization employing Ru (II) sensitizers with anthracene and phenanthrene ancillary ligands

Cite this: DOI: 10.1039/x0xx00000x

Received
Accepted

DOI: 10.1039/x0xx00000x

www.rsc.org/

Hammad Cheema[a], Robert Younts[b], Louis Ogbose[c], Bhoj Gautam[b], Kenan Gundogdu[b], Ahmed El-Shafei[a]*

In this study, intriguing difference caused by structural isomerization based on anthracene and phenanthrene stilbazole type ancillary ligands in Ru (II) sensitizers for dye sensitized solar cells (DSCs) has been investigated using femtosecond transient absorption spectroscopy. Both anthracene and phenanthrene based sensitizers HD-7 and HD-8, respectively, resulted in similar extinction coefficient, photopysical and thermodynamic free energy of electron injection and dye regeneration as measured by UV-Vis, excited state life time and cyclic voltammetry. However, TiO_2 adsorbed HD-7 resulted in up to 45% less photocurrent density than HD-8 although photovoltage was similar owing to comparable thermodynamic characteristics. It was obvious from the measurement of incident photon to current conversion efficiency (IPCE) that excited electrons in HD-7 are prone to internal energy loss before injection into TiO_2 conduction band. Analysis of photo-induced spectral features measured by femtosecond transient absorption spectroscopy showed that excited electrons in HD-7 are prone to ISC (intersystem crossing) much more than HD-8 and those triplet electrons are not being injected in TiO_2 efficiently. Interestingly, from impedance measurements, HD-7 showed higher recombination resistance than HD-8 and N719, but shorter lifetime for electrons injected in TiO_2 conduction band.

1. Introduction

Dye sensitized solar cells (DSCs) are photovoltaic cells that mimics the natural photosynthesis. In a DSC, the dye absorbs the photons and converts those photons to electric charges, which are then extracted to the outer circuit through semiconductor TiO_2, whereas the mediator regenerates the oxidized dye. Sensitizer is the pivotal component in terms of determining the spectral response, color, photocurrent density, long term stability, and thickness of a DSC. Hence since the invention of DSC in the laboratory of Michael Grätzel 1991[1], DSC in general and sensitizers for DSC in specific are the focus of academic research.

Charge separation on the dye/TiO_2 interface is arguably the most critical step to ensure efficient translation of absorbed photons to photocurrent. The theory which is used to predict the rate of electron transfer between two chemical species was developed by Marcus in 1960[2]. The theoretical adaptation of Marcus theory for electron transfer from optically excited sensitizer to the conduction band of wide band metal semiconductor has been reviewed elsewhere[3-5]. However, it is important to mention that the three components that govern the rate of electron injection are (i) electronic coupling between electron donating orbital of sensitizer and electron accepting orbital of semiconductor, (ii) density of states (DOS) in the conduction band of semiconductor and (iii) free energy difference between dye excited state and conduction band edge of the oxide[3-5]. Electron transfer at the dye/TiO_2 interface is even complex, considering the fundamental difference in the discrete molecular state of sensitizer and a continuum of the delocalized bulk states in semiconductor.

During the last decade, extensive studies to understand both efficiency and kinetics of electron injection have been carried out by pump-probe transient absorption [5-10] , time correlated single photon counting (TCSPC)[9-13] and luminescence quenching methods[14-16].

Electron injection from excited sensitizer to TiO_2 conduction band show two main components, ultrafast <100 fs time scale correlated to singlet (^{1}MLCT) injection and slow component with hundreds of picoseconds[5, 17, 18] attributed to triplet (^{3}MLCT) injection. Ardo and Meyer[19] in an elegant review with more than 480 references, summarized meticulously the different electron injection, intramolecular relaxation and recombination pathways and time domains for transition-metal compounds anchored to TiO_2 semiconductor surfaces.

In this study, femto-second pump probe and time correlated single photon counting (TCSPC) techniques were employed to study the anomaly in photovoltaic and IPCE observed for structural isomers based Ru (II) sensitizers HD-7 and HD-8 as shown in Figure 1. Impedance spectroscopy was employed to study the interface properties which have direct correlation with photocurrent and photovoltage as found previously[20,21]. Photovoltaic measurements of current-potential (I-V) curve and IPCE were carried out under AM 1.5 irradiance conditions. It was found that although HD-7 and HD-8 are structurally not very different, both sensitizers when employed in DSC's showed remarkably different I-V and IPCE owing to substantial difference in electron injection and dye/TiO_2 interface properties. The purpose was to qualitatively compare and understand the influence of isomerization on photovoltaic performance of DSC's, without quantitative calculations of kinetic parameters for intersystem crossing (ISC), electron injection from singlet and triplet states, which have been reported and discussed extensively elsewhere[5, 17-19, 22].

2. Results and Discussion

2.1. Photopysical Measurements

For the synthesis of proposed sensitizers HD-7 and HD-8, the corresponding antenna ligands were synthesized first by reaction of relevant aromatic aldehydes and 4,4'-dimethyl-2,2'-bipyridyl in a pressure tube in the presence of excess of chlorotrimethylsilane to produce the corresponding bis-stilbazole in Knoevenagel condensation type reaction [9-13]. The synthetic procedures for the ligands and complexes can be found in SI (supplemental information).

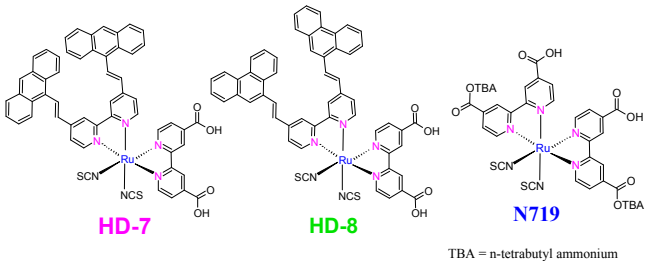

Fig 1. Molecular structures of complexes HD-7 and HD-8.

The proposed Ru (II) sensitizers were then synthesized in the typical one pot three steps synthetic scheme as given in ESI. The yield of the crude products was in the range of 90-95%, which was purified through Sephadex LH-20 column three times to give the highly pure product in 50% yield. The pure product was then characterized by FT-IR, ^{1}H-NMR, and high resolution mass spectrometry ($^-$ESI). The chemical structures of HD-7 and HD-8 are depicted in Figure 1.

The photon harvesting capability of Ru (II) sensitizers can be tuned by the functionalization of the bipyridyl ancillary ligands with extended conjugation or electron donating groups as found previously[13, 23-25]. Ancillary ligands for HD-7 and HD-8 were named LH-7 and LH-8 and are shown in Scheme S1 (Supplementary information). To characterize the photopysical properties of LH-7 and LH-8, absorption and emission were performed and the results are shown in Figure S1. Absorption λ_{max} for LH-7 was 389nmcompared to 346nm of LH-8. Apparently, absorption spectrum of LH-7 is better in terms of harvesting more visible photons. Emission λ_{max} was at 492nm for LH-7 compared to 425nm of LH-8 leading to Stokes shifts of 103nm and 79nm, respectively. Thus, it can be concluded based on stokes shifts that comparatively more energy was lost from excited electrons (most likely by vibrational relaxation or intersystem crossing) before luminescence decay for LH-7 than that of LH-8.

A comparison among the UV-Vis absorption and emission spectra of HD-7, HD-8 and N719, measured in DMF using concentration of 2 x10^{-5} M, is given in Figure 2 and the results are summarized in Table 1.

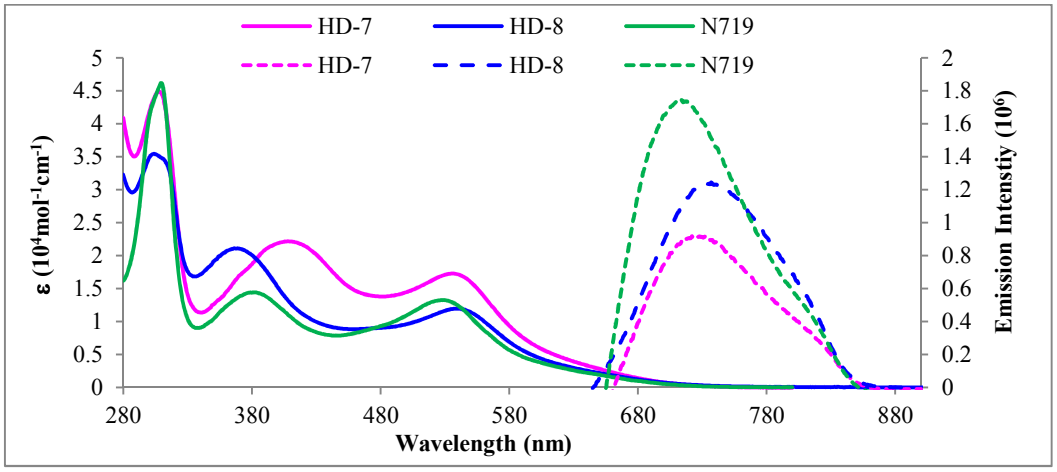

Fig. 2. UV-Vis absorption (solid-line) and emission spectra (dashed-line) of complexes HD-7, HD-8 and N719 measured in DMF (2 x10^{-5}M).

Table 1. Absorption and emission properties for HD-7, and HD-8 compared to N719

Sensitizer	Absorption λ_{max} (nm)	ε (M^{-1} cm^{-1})	Emission, λ_{max} (nm)
HD-7	305,411,533 (d→π*)	44,150; 22,100; 17,200	721
HD-8	300,365,537 (d→π*)	34,750; 21,000; 11,900	730
N719	310,381,529(d→π*)	46 100; 14,400; 12,800	712

In order to study the effect of extended conjugation on excited state lifetime of sensitizers HD-7 and HD-8, time correlated single photon counting (TCSPC) method was employed. Figure S2 (Supplementary information) shows the excited state decay behavior of the dyes. Emission decay lifetime for HD-7, HD-8 and N719 was measured and found to be 31ns, 51ns, and 38ns respectively, as given in Table S1 without purging the solutions with argon. The measured value of excited state lifetime for N719 in air saturated ethanol solution is 40ns[26], which was 38ns as found in DMF for this study.

2.2. Electrochemical Measurements

The comparison between the ground state oxidation potential (GSOP), excited state oxidation potential (ESOP), electron injection and dye regeneration free energy for HD-7, HD-8 and N-719 is shown in Figure 3 and the results are summarized in Table S2. The measurements of GSOP and ESOP by cyclic voltammetry are explained in supplementary information whereas $E_{0\text{-}0}$ was calculated from the onset of absorption spectra. The GSOP values of -5.46 eV, and -5.45 eV for HD-7, and HD-8, respectively confirmed that the HOMO of these dyes are below the I_3^-/I^- redox couple (-5.2 eV) [27], and there is enough thermodynamic driving force for efficient dye regeneration. Additionally, ESOP level of HD-7 and HD-8 were at -3.6 eV and -3.54 eV, respectively, which lay above the conduction band edge of nanocrystalline TiO_2 (-4.2 eV)[28]. Thus owing to the energetically favorable excited states, the efficient electron injection into the CB edge of TiO_2 and dye regeneration was achieved with sensitizers HD-7 and HD-8.

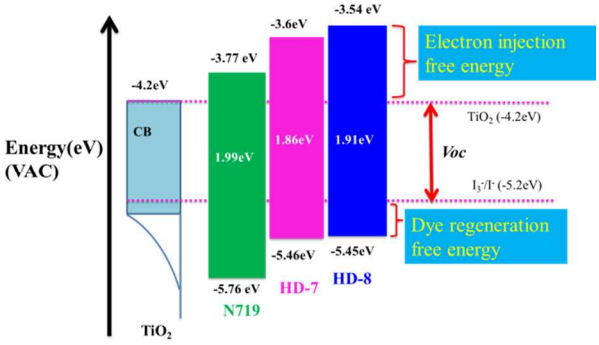

Fig. 3. Energy level diagram and comparison between GSOP and ESOP of N719, HD-7, and HD-8.

2.3. Photovoltaic Device Characterizations

The photovoltaic performance of complexes HD-7 and HD-8 on nanocrystalline TiO_2 electrode was studied under standard AM 1.5 irradiation (100 mW cm^{-2}, one sun illumination). The TiO_2 electrode was prepared by using the method reported by Grätzel et al[29] and details about the steps and the materials used is given in supplemental information.

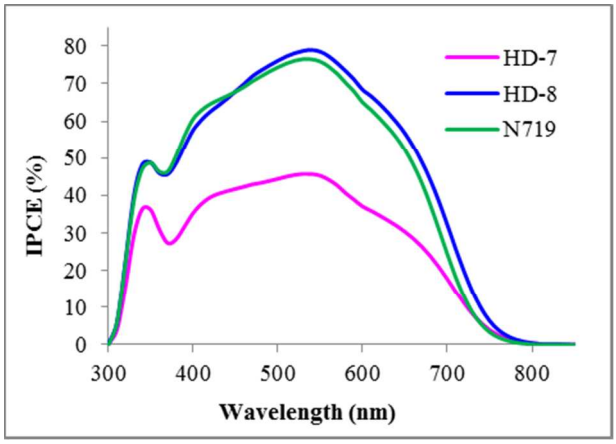

Fig. 4. Photocurrent action spectra (IPCE) obtained with dyes HD-7, HD-8, and N719 anchored on nanocrystalline TiO_2 film.

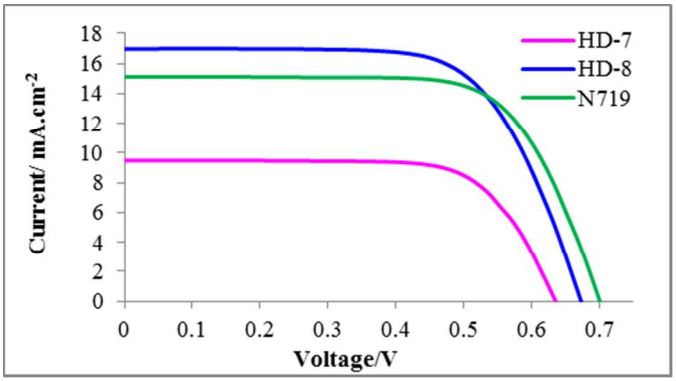

Fig. 5. Photocurrent-voltage characteristics of DSCs sensitized with the complexes HD-7, HD-8 and N719, coadsorbate CDCA 20 mM and electrolyte (Solaronix, Iodolyte AN-50).

Under similar conditions, HD-8 outperformed benchmark N719 in terms of incident-photon to current conversion efficiency (IPCE) response in the wavelength range of 450-800nm as shown in Figure 4. IPCE response as high up to 79% was achieved for HD-8 compared to 76% of N719. Better IPCE response by HD-8 can be attributed to extended conjugation by incorporation of stilbazole and phenanthrene in the ancillary ligand. In comparison, IPCE response by HD-7 was poor, though both HD-7 and HD-8 employ very similar strategy for extension of conjugation. In a similar Ru (II) sensitizer (MH11) [30] by employing pyrene instead of phenanthrene, El-Shafei *et al* attributed the higher IPCE and J_{sc} to the highly conjugated, bulky and hydrophobic nature of the ancillary ligand. Similarly, phenanthrene and anthracenec-based ancillary ligands were expected to offer a barrier to recombination or loss of excited electrons by combining with oxidized dye or electrolyte. According to IPCE results, phenanthrene performs as anticipated whereas anthracene was far poor in photocurrent response than expected. Similar results for I-V curve were obtained which are shown in Figure 5.

Table 2 summarizes the photovoltaic parameters including the short-circuit photocurrent density (J_{sc}), open-circuit voltage (V_{oc}), fill factors (*ff*) and overall cell efficiencies (η, *%*).

Table 2. Photovoltaic characteristics of HD-7, HD-8 and N719

Sensitizer	J_{sc}(mA cm^{-2})	V_{oc} (V)	FF	η (%)
HD-7	9.48	0.65	0.72	**4.4**
HD-8	16.96	0.68	0.68	**7.9**
N719	15.1	0.71	0.71	**7.6**

J_{sc}, short-circuit photocurrent density; V_{oc}, open-circuit photovoltage; FF, fill factor; η, total power conversion efficiency. TiO_2 active area 0.18cm^{-2}

HD-8 outperformed other two sensitizers by resulting in J_{sc} of 16.96 mA cm^{-2} and V_{oc} of 0.68V. Superior IPCE response of HD-8 translated into higher J_{sc} than HD-7 and N719. The overall η (%) for HD-8 was 7.9 compared to 4.4 of HD-7 and 7.6 of N719 under similar conditions. The overall better photovoltaic parameters of HD-8 can be attributed to thermodynamically more favorable ground and excited state properties than N719. On the other hand, poor IPCE response of HD-7 translated into low J_{sc} of 9.48 mA cm^{-2}. Though HD-7 have thermodynamically favorable redox properties, the poor performance in DSC can be attributed to the internal loss of excited electrons either through recombination or intersystem crossing since V_{oc} of HD-7 is not substantially lower than HD-8. In order to rationalize the excited electrons loss for HD-7, femtosecond transient absorption and impedance measurements were performed.

2.4. Electrochemical Impedance Spectroscopy Characterization

Electrochemical Impedance Spectroscopy (EIS) is a powerful tool which gives the phase and magnitude of response as the fuction of modulation in frequency of voltage. This then leads to analysis and measurement of appropriate transfer functions. In DSC, EIS can be used effectively to charectrize the interfacial charge transfer process at TiO_2/dye, pt/electrolyte and predict electron lifetime in TiO_2

conduction band[20, 21, 31, 32]. The combination of charge transfer resistance and chemical capacitance give rise to a semicircle at the complex plan. The EIS Nyquist and Bode plots for the DSCs based on HD-7, HD-8 and N719 are shown in Figures 6 and 7. In EIS Nyquist plots, the electron recombination resistance was in the order HD-7>N719>HD-8. Although, the order of radius size for the semicircle is usually consistent with V_{oc} obtained [20, 21, 31, 32] from devices, however anomaly in HD-7 recombination resistace was observed. Similar anomaly in the form of higher recombination resistance was observed and reported previously for sensitizers[13, 33] which favor triplet state injection while anchored to TiO_2.

In Figure 7, the frequency response in the range of 0 to 2.5 Log/Hz, is related to the electron lifetime in the CB of TiO_2 ($eTiO_2$). In essence, Bode plot compliments Nyquist plot and the sensitizer which offers the highest resistance at TiO_2 surface for charge recombination with electrolyte shows the highest phase change peak shifted towards lower frequency[13, 22]. In this case, the frequency (0-2.5 Log/Hz) peak of the DSCs based on N719 and HD-8 was shifted to lower frequency relative to that of HD-7 indicating a shorter recombination lifetime for HD-7, thus resulting in lower V_{oc} for HD-7 compared to N719 and HD-8 as given in Table 2 for solar cells.

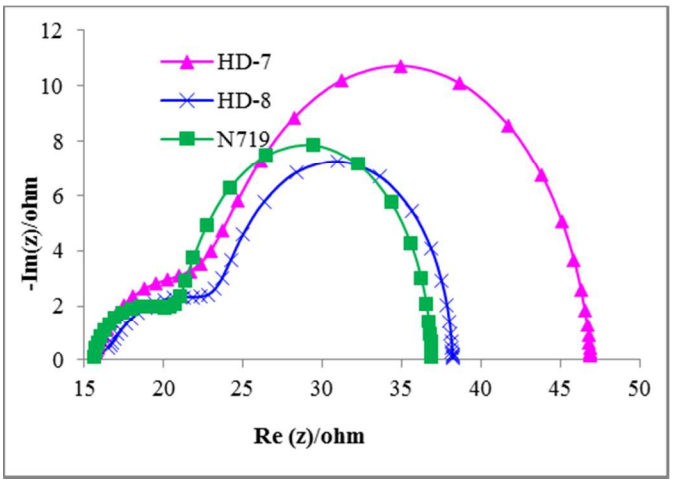

Fig. 6. EIS Nyquist plots for DSCs sensitized with HD-7, HD-8, and N719.

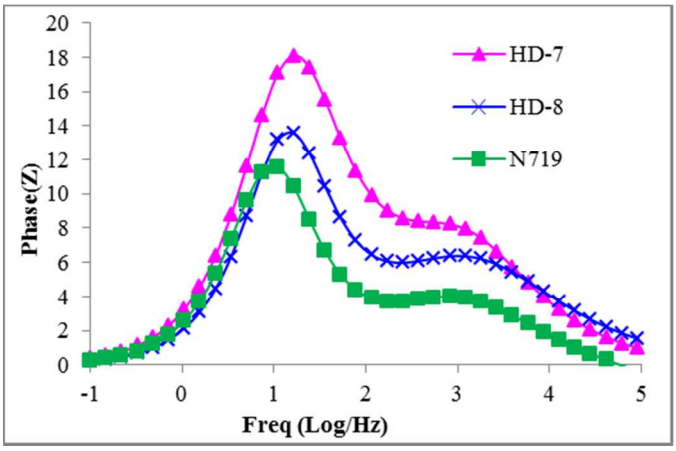

Fig. 7. EIS Bode plots for DSCs sensitized with HD-7, HD-8, and N719.

The injected electron lifetime $eTiO_2$ can be determined by using the relation ($\tau_{CB} = 1/2\pi f$), where τ is the lifetime of electrons in TiO_2 and f is mid frequency peak in Bode plots. The frequency peak of the DSCs based on HD-7, HD-8 and N719 were at 90Hz, 84Hz, and 18Hz, corresponding to eTiO2 of 1.76ms, 1.9ms and 8.8 ms, respectively, thus resulting in lower V_{oc} for HD-7 and HD-8 compared to N719, which correlates well with the actual V_{oc} reported for the solar cells

Anomaly in the form of higher recombination resistance observed in the Nyquist plot of HD-7 and poor IPCE response shows that the excited electrons are in a state which either hinders the charge difussion (both on TiO_2 surface and in recombination with electrolyte) or the excited electrons are going through internal loss such as higher intersystem crossing.

2.5. Femtosecond Transient Absorption Spectroscopy Measurements

Femtosecond Transient Absorption Spectroscopy (TAS) was employed to investigate the early charge injection dynamics in HD-7 and HD-8 films and understand the underlying causes which result in such a drastic difference in short circuit current density (J_{sc}). TA spectra for HD-7 and HD-8 films with the addition of an iodide-based electrolyte are shown in Figures 8(a) and 8(b), respectively. The spectra show negative ground state bleaching (GSB) features, which result from a decrease in absorption in the excited (pumped) dye, less than 620nm (> 2.0eV). The spectra is dominated by a broad photo-induced absorption (PA) band, which results from increased absorption of the excited (pumped) dye, greater than 620nm (< 2.0eV). This broad PA band is the convolution of two PA spectral features. We attribute one PA feature to the absorption of the excited-state dye (dye*) at approximately 650 nm, and the other

to the absorption of the oxidized-dye (dye$^+$) at approximately 760 nm, which is in agreement with previous studies on Ru(II) based DSCs[6, 8, 12, 18, 19, 34-37]. The oxidized-dye is formed after charge injection occurs, and is therefore a probe of the ultrafast charge injection dynamics in DSCs [6, 8, 12, 18, 19, 34-37]. It is important to note in (Figure 8) that in HD-7 film, after 500 ps, at 760 nm (dye$^+$) there is a large increase in the PA signal while at 650 nm (dye*) the PA signal is unchanged. In contrast, after 500 ps, in the HD-8 film the PA band at 760 nm (dye$^+$) decreases slightly while the PA signal at 650 nm (dye*) decreases significantly. Comparison of TA spectra for HD-7 and HD-8 at 1ps and 500ps in the presence of electrolyte is shown in Figure S10.

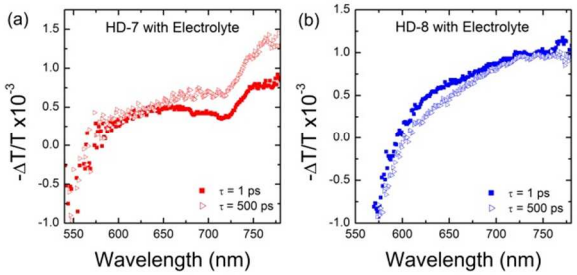

Figure. 8. Transient Absorption spectra for (a) HD-7 (b) HD-8 films with the addition of the iodide-based electrolyte at 1 ps and 500 ps delay time, whereas samples were excited with 100 fs pulses tuned at 530 nm

To understand the significant differences in the spectral evolution in HD-7 and HD-8, we compared the time evolution of the dye* and dye$^+$ PA bands in films with and without the addition of the electrolyte as shown in Figure 9. It has been shown previously [12] that the electrolyte solution can shift the energy of the conduction band in TiO_2 and as a result can affect the charge injection dynamics. It has also been shown previously[9, 18, 38] in similar Ru(II) DSCs that the slow secondary rise of dye$^+$ can be attributed to charge injection from the triplet MLCT states (^{3}MLCT) and occurs over pico to ns timescales, similar to that of HD-7. Thus addition of the electrolyte solution favors additional charge injection pathways to form. Therefore, on the addition of electrolyte to the HD-7 and HD-8 films, the dye$^+$ TA signal increases due to the increase in injection from both singlet and triplet MLCT states.

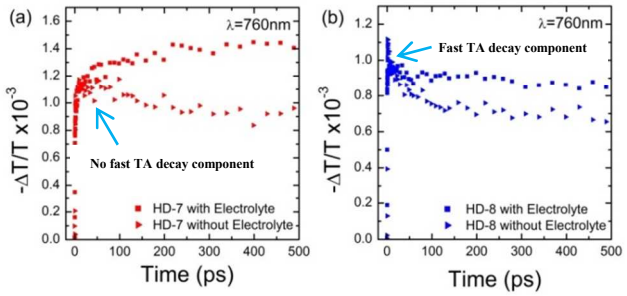

Figure. 9. Time evolution of the TA spectra of the oxidized-dye (dye$^+$) at 760 nm for (a) HD-7 films with and without the electrolyte solution and (b) HD-8 films with and without the electrolyte solution. Films were excited with 100 fs pulses tuned at

530 nm.However, HD-7 shows significantly larger TA signal related to oxidized triplet state than HD-8 (Figure 9), which suggests that either HD-7 has a significantly larger proportion of initially filled ^{3}MLCT states or has higher ISC rate to triplet state than HD-8. As a result, HD-7 has less singlet charge injection (^{1}MLCT) and preferred slow triplet charge injection (^{3}MLCT) for which free energy of electron injection is lower. In contrast, the dominate charge injection pathway for HD-8 is through singlet injection (^{1}MLCT), which is confirmed due to the presence of fast sharp decay in TA signal of HD-8 (Figure 9b), whereas no such fast sharp TA decay component was observed for HD-7 (Figure 9a). Since the free energy of injection is larger for singlet state than triplet state pathway, thus charge injection from the ^{1}MLCT states are likely to contribute more to the current density of the device. The significantly larger proportion of singlet injection in HD-8 than HD-7 correlates well with drastically large increase in short circuit current density in HD-8 than HD-7. Further studies are underway to understand why HD-7 prefers ISC or internal excited electrons loss compared to HD-8 and either this only happens when HD-7 is anchored on TiO_2 or HD-7 show similar behavior in solution. This will eventually help to understand and compare the ultrafast events on the interface and photophysics in solution as a function of isomerization.

3.6. Time Correlated Single Photon Counting (TCSPC) Measurements

In TCSPC, emitted photons are counted and photon arrival time is recorded, which represents the luminescence decay as the function of time [39, 40] which depends on the lifetime of the excited state. For DSCs, TCSPC method [9-13] can be employed to study the emission

decay behavior of dyes anchored to TiO_2, particularly in the presence of electrolyte which retards the kinetic processes due to electrolyte induced shifts in the dye-TiO_2 system[3, 5, 12, 35, 41].

For this study, similar films as employed in femtosecond TAS were used in the presence of electrolyte and the resulted decay curves are shown in Figure 10.

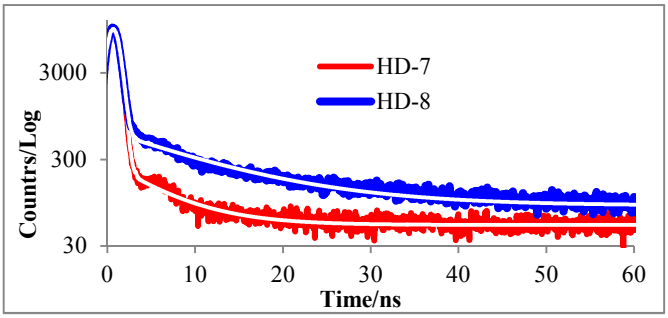

Figure 10. Excited state decay behaviors of HD-7 andHD-8, films were excited with 460nm NanoLED from Horiba with pulse width of 1.3ns, smooth lines correspond to the fits of the experimental data after convolution with the instrument response.

It is obvious from the decay curves of Figure 10 that under similar measurement conditions and film preparation the signal intensity of decay curves for the same number of counts was much less for HD-7 compared to HD-8, showing the difference in population of excited state contributing to radiative and non-radiative transitions. Population of excited state contributing to radiative transitions was significantly higher for HD-8 than HD-7 based film. This unambiguously concludes that in the presence of electrolyte, HD-7 favor raditionless loss of excited electrons, which was established by femtosecond TAS experiments.

4. Conclusions

In summary, this study showcases the crucial findings related to role of triplet state and ultrafast singlet electron injection for Ru(II) sensitizers in DSCs. HD-7 employing anthracene based ancillary ligand was found to be prone to ISC before singlet injection into TiO_2 as found by femtosecond TAS. In femtosecond TAS, time evolution of the transient absorption signal of the oxidized dye clearly shows dominant presence of triplet state oxidized form for HD-7 compared to HD-8. However, the observed dominant triplet state in TiO_2 for HD-7 do not translate to photocurrent efficiently, due to lack of enough thermodynamic driving force for electron injection caused by low energy of triplet state whereas dominate charge injection pathway for HD-8 is through singlet injection (^{1}MLCT) as found by femtosecond TAS. Impedance and TCSPC measurements comparison for employed sensitizers favors the conclusion of raditionless loss of excited electrons for HD-7 compared to HD-8. This raditionless loss of energy is most probably related to ISC for Ru (II) HD-7 sensitizer with anthracene ancillary ligand. The findings of this study support the dominant role of fast singlet injection for HD-8 compared to less efficient slow triplet state injection of HD-7.

Notes and references

[a]Polymer and Color Chemistry Program, North Carolina State University, Raleigh, NC, 27695, USA.
[b]Physics Department, North Carolina State University, Raleigh, NC, 27695, USA.
[c] Ahmadu Bello University, Zaria, Nigeria.

† Electronic Supplementary Information (ESI) available: Synthesis details, FT-IR, High-Resolution ESI-MS, ^{1}H-NMR and cyclic voltammetry graphs are given as Supporting Information.

References

1 B. O'Regan and M. Grätzel, Nature, 1991, 353, 737-740.
2 R. A. Marcus, J. Chem. Phys., 1965, 43, 679-701.
3 J. B. Asbury, E. Hao, Y. Wang, H. N. Ghosh and T. Lian, J Phys Chem B, 2001, 105, 4545-4557.
4 N. A. Anderson and T. Lian, Coord. Chem. Rev., 2004, 248, 1231-1246.
5 J. J. H. Pijpers, R. Ulbricht, S. Derossi, J. N. H. Reek and M. Bonn, J. Phys. Chem. C, 2011, 115, 2578-2584.
6 G. Benko, J. Kallioinen, J. Korppi-Tommola, A. P. Yartsev and V. Sundstram, J. Am. Chem. Soc., 2002, 124, 489-493.
7 B. Wenger, M. Grätzel and J. Moser, J. Am. Chem. Soc., 2005, 127, 12150-12151.
8 Y. Tachibana, J. E. Moser, M. Grätzel, D. R. Klug and J. R. Durrant, J. Phys. Chem., 1996, 100, 20056-20062.
9 H. Cheema, A. Islam, L. Han, B. Gautam, R. Younts, K. Gundogdu and A. El-Shafei, J. Mater. Chem. A, 2014, 2, 14228-14235.
10 L. J. Antila, P. Myllyperkio, S. Mustalahti, H. Lehtivuori and J. Korppi-Tommola, J. Phys. Chem. C, 2014, 118, 7772-7780.
11 S. E. Koops and J. R. Durrant, Inorg. Chim. Acta, 2008, 361, 663-670.
12 S. A. Haque, E. Palomares, B. M. Cho, A. N. M. Green, N. Hirata, D. R. Klug and J. R. Durrant, J. Am. Chem. Soc., 2005, 127, 3456-3462.
13 H. Cheema, A. Islam, L. Han and A. El-Shafei, ACS Appl. Mater. Interfaces, 2014, 6, 11617-11624.
14 R. W. Fessenden and P. V. Kamat, J. Phys. Chem., 1995, 99, 12902-12906.
15 O. Bräm, F. Messina, A. M. El-Zohry, A. Cannizzo and M. Chergui, Chem. Phys., 2012, 393, 51-57.
16 O. Bram, A. Cannizzo and M. Chergui, Phys. Chem. Chem. Phys., 2012, 14, 7934-7937.
17 B. Braggemann, J. A. Organero, T. Pascher, T. Pullerits and A. Yartsev, Phys. Rev. Lett., 2006, 97, 208301.
18 A. Furube, Z. Wang, K. Sunahara, K. Hara, R. Katoh and M. Tachiya, J. Am. Chem. Soc., 2010, 132, 6614-6615.
19 S. Ardo and G. J. Meyer, Chem. Soc. Rev., 2009, 38, 115-164.

20 N. Koide, A. Islam, Y. Chiba and L. Han, J. Photochem. Photobiol. A., 2006, 182, 296-305.
21 A. El-Shafei, M. Hussain, A. Islam and L. Han, J. Mater. Chem. A, 2013, 1, 13679-13686.
22 J. Kallioinen, G. Benko, V. Sundstrom, J. Korppi-Tommola and A. P. Yartsev, *J Phys Chem B,* 2002, **106,** 4396-4404
23 D. Shi, N. Pootrakulchote, R. Li, J. Guo, Y. Wang, S. M. Zakeeruddin, M. Grätzel and P. Wang, J. Phys. Chem. C, 2008, 112, 17046-17050.
22 24 N. Onozawa-Komatsuzaki, M. Yanagida, T. Funaki, K. Kasuga, K. Sayama and H. Sugihara, Inorganic Chemistry Communications, 2009, 12, 1212-1215.
25 A. El-Shafei, M. Hussain, A. Atiq, A. Islam and L. Han, J. Mater. Chem., 2012, 22, 24048-24056.
26 M. K. Nazeeruddin, S. M. Zakeeruddin, R. Humphry-Baker, M. Jirousek, P. Liska, N. Vlachopoulos, V. Shklover, C. Fischer and M. Grätzel, Inorg. Chem., 1999, 38, 6298-6305.
27 G. Oskam, B. V. Bergeron, G. J. Meyer and P. C. Searson, J Phys Chem B, 2001, 105, 6867-6873.
28 A. Hagfeldt and M. Graetzel, Chem. Rev., 1995, 95, 49-68.
29 S. Ito, T. N. Murakami, P. Comte, P. Liska, C. Grätzel, M. K. Nazeeruddin and M. Grätzel, Thin Solid Films, 2008, 516, 4613-4619.
230 M. Hussain, A. El-Shafei, A. Islam and L. Han, Phys. Chem. Chem. Phys., 2013, 15, 8401-8408.
31 M. Adachi, M. Sakamoto, J. Jiu, Y. Ogata and S. Isoda, J Phys Chem B, 2006, 110, 13872-13880.
32 L. Han, N. Koide, Y. Chiba, A. Islam and T. Mitate, Comptes Rendus Chimie, 2006, 9, 645-651.
33 H. Cheema, A. Islam, L. Han, B. Gautam, R. Younts, K. Gundogdu and A. El-Shafei, J. Mater. Chem. A, 2014, 2, 14228-14235.
34 R. Katoh, A. Furube, M. Kasuya, N. Fuke, N. Koide and L. Han, J. Mater. Chem., 2007, 17, 3190-3196.
35 S. E. Koops, B. C. O'Regan, P. R. F. Barnes and J. R. Durrant, J. Am. Chem. Soc., 2009, 131, 4808-4818.
36 J. Sobus, G. Burdzinski, J. Karolczak, J. Idigoras, J. A. Anta and M. Ziolek, Langmuir, 2014, 30, 2505-2512.
37 J. Teuscher, J. DÃ©coppet, A. Punzi, S. M. Zakeeruddin, J. Moser and M. Grätzel, J. Phys. Chem. Lett., 2012, 3, 3786-3790.
38 A. Hagfeldt, G. Boschloo, L. Sun, L. Kloo and H. Pettersson, Chem. Rev., 2010, 110, 6595-6663.
39 B. Valeur 1944-, Molecular Fluorescence : Principles and Applications, Wiley-VCH, Weinheim, 2002.
40 J. R. Lakowicz, Principles of Fluorescence Spectroscopy, Springer, New York, 2006.
41 Y. Tachibana, S. A. Haque, I. P. Mercer, J. E. Moser, D. R. Klug and J. R. Durrant, J Phys Chem B, 2001, 105, 7424-7431.

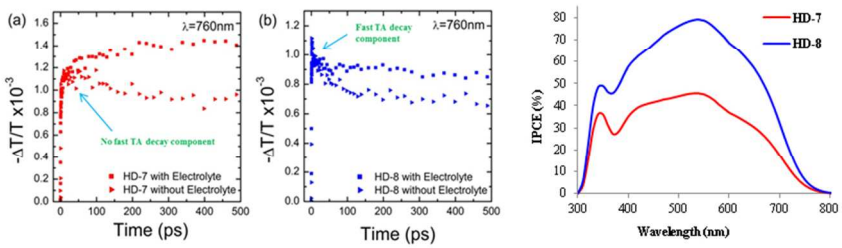

HD-7, prone to ISC, continuous increase in triplet TA signal
HD-8, enhanced singlet injection, followed by decay in TA signal